自動導航車超音波感測定位系統

林鴻興、蔡清池

摘要

本文提出自動導航車超音波感測之自我定位方法，使用兩個超音波發射器及三個接收器之超音波飛行時間(Time of flight)測量法，這種定位方法皆能決定自動導航車相對於參考座標的絕對位置及車頭方向。透過電腦模擬及實驗數據足以證明本論文所提方法的有效性與可行性。

關鍵詞：自動導航車，定位，超音波感測，飛行時間。

林鴻興：修平技術學院電機工程系講師
蔡清池：中興大學電機系教授

A Localization System of a Mobile Robot Using Ultrasonic Measurements

Hung-Hsing Lin, Ching-Chih Tsai

Abstract

Based on ultrasonic sensory information, an approach based on ultrasonic time-of-flight (TOF) data is proposed for localization of an autonomous mobile robot (AMR). It will be proven that the combination of two ultrasonic transmitters and three receivers can be used to determine both the position and the orientation of an AMR with respect to a world frame uniquely. A series of simulation and experimental results are provided to show the validity and feasibility of the proposed methods.

Keywords: autonomous mobile robots, localization, ultrasonic sensors, time-of-flight.

Hung-Hsing Lin : Instructor, Department of Electrical Engineering, HIT
Ching-Chih Tsai : Professor, Department of Electrical Engineering, National Chung Hsing University

1. Introduction

Navigation of the autonomous mobile robots (AMRs) usually needs two kinds of sensor systems whose functions can complement each other. The first one is the use of the internal sensing systems or methods that have been widely used for most wheeled mobile robots to calculate their current locations with respect to an inertial frame of reference. Such sensors include encoders, speedometers, rate-gyros, tilt sensors and so on. The type of navigation system can be achieved by the dead-reckoning(DR) method or the inertial navigation system(INS) [1-3]. The second one is the external sensing systems that provide temporal or spatial information obtained from the vehicle to its surrounds. The most prevalent external sensors are digital compasses, ultrasonic ranging sensors, vision systems, Differential Global Position System(DGPS) and so on. Each kind of sensing system has its strong points and drawbacks due to the operation environments. The selection of the navigation sensors depends upon price, desired measurement range and accuracy [4,5].

AMRs have already found widespread applications in automated factories, offices, hospitals and warehouses, It can be permitted to install the sensing equipment on a special environmental space, in order to describe the environmental modeling and to provide accurate absolute locations for the autonomous mobile robots. In the outdoor environment, the use of sensor equipment is quite different from the obvious road mark or the beacons of robots operation environment. Due to the very properties of ultrasonic sensors, such as low-cost, and noncontactness , the purpose of this paper is to design a novel self-localization of autonomous mobile robots.

Wu and Tsai [6] used three ultrasonic transmitters and two receivers to find the localization and orientation of an autonomous mobile robot based on ultrasonic sensory information. Tsai [7] developed a novel location system for an autonomous mobile robot designed to perform missions in any given structured environment. Its hardware consists of a multisensorial dead- reckoning subsystem, a modified ultrasonic location subsystem, and a host PC 586 computer. However, the proposed system in [7] suffers difficulties of finding initial position and orientation of an AMR. The aim of the paper is to combine the techniques proposed in [6] and [7] for developing a new type of location system. This novel location system not only provides an initial position and orientation information for the AMR, but also determines the dynamic robot position and orientation information [8,9].

The outline of the paper is organized as follows. Section 2 shows the mathematical frame of the location system. Section 3 describes the hardware configuration of the location system. Several computer simulations and experimental results for self-localization of the AMR are shown in Section 4. Conclusions of the paper are given in section 5.

2. Mathematical Frame of the Location System

This section presents a hardware configuration and an approach for self-localization of the AMR using mere ultrasonic measurements. Figure 1 depicts the physical configuration of the novel ultrasonic location system, which consists of two RF controlled ultrasonic transmitters installed at the known position with respect to the reference frame, two sets of RF controlled switches operating in different frequencies, and three ultrasonic receivers placed on the AMR. In order to measure the time-of-flight (TOF) data between the ultrasonic transmitter/receiver modules, the computer selects and drives one ultrasonic transmitter by means of one RF controlled switch to send modulated signal. Simultaneously, each 16-bit counter with a 2 MHz counting rate accumulates the TOF data until the corresponding receiver confirms that the ultrasonic modulated signal has been received. The ultrasonic transmitters can be installed at any arbitrary position with respect to the reference frame, but it is constrained by that the two transmitters must be installed at the same height along the z-axis and the distance between them must be suitable (about 15-20 cm). The geometric arrangement of the receivers mounted on the robot is shown in Figure 2, in which three receivers are installed at the same height on the robot.

Suppose that two ultrasonic transmitters are installed at the known positions T1:(x_{t1}, y_{t1}, z_t) and T2:(x_{t2}, y_{t2}, z_t) and three receivers' locations are denoted by R1:(x_1, y_1, z), R2:(x_2, y_2, z) and R3:(x_3, y_3, z), respectively. Then the pose of the robot, represented by (x, y, z,θ), can be determined uniquely by the distances from the transmitters to receivers. Let d_1, d_2, ...,d_6 denote the distances from the points (x_{t1}, y_{t1}, z_t) and (x_{t2}, y_{t2}, z_t) to the points(x_1, y_1, z), (x_2, y_2, z) and (x_3, y_3, z), respectively. Then one will obtain

$$(x_1 - x_{t1})^2 + (y_1 - y_{t1})^2 + (z - z_t)^2 = d_1^2 \quad (1)$$

$$(x_1 - x_{t2})^2 + (y_1 - y_{t2})^2 + (z - z_t)^2 = d_2^2 \quad (2)$$

$$(x_2 - x_{t1})^2 + (y_2 - y_{t1})^2 + (z - z_t)^2 = d_3^2 \quad (3)$$

$$(x_2 - x_{t2})^2 + (y_2 - y_{t2})^2 + (z - z_t)^2 = d_4^2 \quad (4)$$

$$(x_3 - x_{t1})^2 + (y_3 - y_{t1})^2 + (z - z_t)^2 = d_5^2 \quad (5)$$

$$(x_3 - x_{t2})^2 + (y_3 - y_{t2})^2 + (z - z_t)^2 = d_6^2 \quad (6)$$

From Figure 1, let the mobile robot's location be denoted by (x, y, z), whose geometric relations to the position of the receivers R1, R2 and R3 are expressed by

$$\begin{cases} x_1 = x + b\cos\theta \\ y_1 = y + b\sin\theta \end{cases} \quad (7)$$

$$\begin{cases} x_2 = x + b\sin\theta \\ y_2 = y - b\cos\theta \end{cases} \quad (8)$$

$$\begin{cases} x_3 = x - b\sin\theta \\ y_3 = y + b\cos\theta \end{cases} \quad (9)$$

where b represents the distance from the location (x, y, z) to each receiver and θ is the robot heading angle.

After manipulating some complicated calculations, we can obtain x_1 and y_1 from Eqs. (1-6) and (7-9).

$$x_1 = \frac{1}{4b[(y_{t2}-y_{t1})\sin\theta + (x_{t2}-x_{t1})\cos\theta]}[2b\cos\theta \times (d_1^2 - d_2^2 + x_{t2}^2 - x_{t1}^2 + y_{t2}^2 - y_{t1}^2) + (y_{t2}-y_{t1}) \times (d_3^2 - d_5^2 + 4bx_{t1}\sin\theta - 4by_{t1}\cos\theta)] \quad (10)$$

$$y_1 = \frac{1}{4b[(y_{t2}-y_{t1})\sin\theta + (x_{t2}-x_{t1})\cos\theta]}[2b\sin\theta \times (d_1^2 - d_2^2 + x_{t2}^2 - x_{t1}^2 + y_{t2}^2 - y_{t1}^2) - (x_{t2}-x_{t1}) \times (d_3^2 - d_5^2 + 4bx_{t1}\sin\theta - 4by_{t1}\cos\theta)] \quad (11)$$

where

$$\cos\theta = \frac{1}{4b[(x_{t2}-x_{t1})^2 + (y_{t2}-y_{t1})^2]}[(y_{t2}-y_{t1}) \times (d_5^2 - d_6^2 - d_3^2 + d_4^2) + (x_{t2}-x_{t1}) \times (2d_1^2 - 2d_2^2 - d_3^2 - d_5^2 + d_4^2 + d_6^2)] \quad (12)$$

$$\sin\theta = \frac{1}{4b[(x_{t2}-x_{t1})^2 + (y_{t2}-y_{t1})^2]}[(x_{t1}-x_{t2}) \times (d_5^2 - d_6^2 - d_3^2 + d_4^2) + (y_{t2}-y_{t1}) \times (2d_1^2 - 2d_2^2 - d_3^2 - d_5^2 + d_4^2 + d_6^2)] \quad (13)$$

Moreover, substituting the values of x_1 and y_1 into Eq. (1) will give

$$z = z_t \pm \sqrt{d_1^2 - (x_1 - x_{t1})^2 - (y_1 - y_{t1})^2} \quad (14)$$

According to the relative position of the transmitter and receiver, the value of z can be determined from one of the two possible values in Eq. (14). Furthermore, substituting the values of x_1 and y_1 into Eq. (7) gives

$$x = x_1 - b\cos\theta \quad (15)$$

$$y = y_1 - b\sin\theta \quad (16)$$

Finally, From Eqs. (12-13), we obtain the orientation θ of the vehicle as follows

$$\theta = \begin{cases} 0 & ,\cos\theta > 0, \sin\theta = 0 \\ \pi/2 & ,\cos\theta = 0, \sin\theta > 0 \\ 3\pi/2 & ,\cos\theta = 0, \sin\theta < 0 \\ \pi & ,\cos\theta < 0, \sin\theta = 0 \\ \tan^{-1}\dfrac{\sin\theta}{\cos\theta} & ,\cos\theta > 0, \sin\theta > 0 \\ \tan^{-1}\dfrac{\sin\theta}{\cos\theta} + \pi & ,\cos\theta < 0, \sin\theta > 0 \\ \tan^{-1}\dfrac{\sin\theta}{\cos\theta} + \pi & ,\cos\theta < 0, \sin\theta < 0 \\ \tan^{-1}\dfrac{\sin\theta}{\cos\theta} + 2\pi & ,\cos\theta > 0, \sin\theta < 0 \end{cases} \quad (17)$$

$where\ \tan^{-1}(\cdot) \in (-\pi/2, +\pi/2)$

This completes the derivation of the position and orientation of the robot from the six ultrasonic measurements and geometric relations of the receivers[10].

3. Hardware Configuration

The physical configuration of the proposed location system is shown in Figure 3, in which two ultrasonic transmitters are installed at positions [0,0,0], [0,a,0] of the reference frame, respectively, and three receivers are mounted on the AMR. The only requirement is that the three receivers must be installed at the same height along the z-axis.

In addition to the two transmitter modules and the three receiver modules, the hardware of the location system also contains a pair of RF controlled switches and a PC-based controller as depicted in Figure 4. The first RF controlled switch sends a radio signal to the corresponding receiver and the personal computer counter starts the counting of the TOF. Once the RF receiver receives the radio signal, the ith ultrasonic transmitter module will send ultrasonic pulses back to the jth receiver immediately in Figures 5 and 6. In this manner, if the distance between the *i*th transmitter and the *j*th receiver is denoted by d_{ij} , then one will obtain

$$TOF_{ij} = \frac{d_{ij}}{V_E} + \frac{d_{ij}}{V_U}, i=1,2,\ j=1,2,3 \qquad (18)$$

where TOF_{ij} is the time-of-flight (TOF) between the ith transmitter and the jth receiver, and V_E and V_U denote the speeds of the electromagnetic wave and the ultrasonic wave, respectively. However, since V_E is much larger than V_U in practice, (18) can be further simplified to be

$$TOF_{ij} = \frac{d_{ij}}{V_U} \qquad (19)$$

Performing the above procedure repeatedly, the values of d_{ij} , $1 \leqq i \leqq 2$, $1 \leqq j \leqq 3$, will be determined sequentially.

4. Simulation, Experimental Results and Discussion

In this simulation, it is assumed that the two ultrasonic transmitters are installed at $(x_{t1}, y_{t1}, z_t)=(15, 12, 190)$ and $(x_{t2}, y_{t2}, z_t) = (20, 28, 190)$ with respect to the reference frame. The TOF measurements are mixed with noise modeled as zero-mean white Gaussian processes with the standard deviation $\sigma_v = 2.5\mu s$. The true position and orientation of the AMR is $(x, y, z, \theta)=(10, 20, 5, 130°)$. Applying the static localization estimation algorithm, the history of the estimated position and orientation of the robot are depicted in Figures 7 and 8, respectively. In Figure 7, the circle is the true position, the cross sign inside the circle denotes the estimated position. Similar results can be shown in Figure 8. It is explicit that the estimates are very close to the true values, and the detailed estimates are $(\hat{x}, \hat{y}, \hat{z}, \hat{\theta}) =$ (9.91, 20.21, 5.07, 130.71°)

The following experiment was performed to investigate the accuracy and precision of the proposed method for static pose estimation of the AMR. Figure 9 display the actual ultrasonic transmitters and receivers. The detailed circuit diagram is shown in Figures 10 and 11. The two ultrasonic transmitters were installed at the positions (x_{t1}, y_{t1}, z_t)=(0, 0, 256) and (x_{t2}, y_{t2}, z_t)=(15, 11, 256) (unit: cm) with respect to the world coordinate reference system, and the spaced distance of the receiver was measured as b=20㎝. While the experiment was being performed, the mean ambient temperature was fixed to be almost constant (T_a=26.4℃) with small temperature fluctuations allowed ($\Delta T_a = \pm 0.3$ ℃), and the correct speed of the ultrasonic wave was 34695.137 ㎝/s [10]. The true position of the robot was (x, y, z)=(0, 0, 46) (unit: cm) with respect to the reference frame, and the heading angle θ were 0°, 45°, 90°, 135°, 180°, 225°, 270° and 315°, respectively. The experimental results are given in Table 1. It is observed by statistics that the ultrasonic location system is proved to be capable of having position accuracy of less than 3 ㎝ and heading accuracy of less than 3°. Although the heading angles are different, the optimal position and orientation estimates of the AMR are all very close to the actual values, which verifies that the proposed system provides highly accurate and reliable estimates.

5. Conclusions

This paper has developed a novel ultrasonic localization system of an AMR in any 3D environment. The physical configuration of the system consists of two RF controlled ultrasonic transmitters installed at known positions, controlled by two sets of RF control switches, and three ultrasonic receivers mounted on the AMR. When the AMR stops inside the effective coverage area of ultrasonic wave propagation, the position and orientation of the robot can be determined uniquely with respect to the world frame by the proposed method. The static localization experimental results have verified that the proposed method provides highly accurate and reliable pose estimates of the robot.

6. References

[1]. T. Fukao, H. Nakagawa, and N. Adachi "Adaptive Tracking Control of a Nonholonomic Mobile Robot," IEEE Transactions on Robotics and Automation, vol. 16, no. 5, pp. 609-615, October 2000.

[2]. D. Maksarov, and H. Durrant- Whyte, "Mobile vehicle navigation in unknown environments: A multiple hypothesis approach", IEEE Proc. Contr. Appl. Theory, vol. 142, no. 4, pp. 385-400, 1995.

[3]. M. Drumheller, "Mobile robot location using sonar", IEEE Trans. Pattern Anal. Machine Intell., vol. PAMI-9, pp. 325-332, Mar. 1987.

[4]. J. J. Leonard, and H. F. Durrant- Whyte , "Directed Sonar Sensing for Mobile Robot Navigation", Boston/London /Dordrecht:Kluwer,1992.

[5]. B. Triggs, "Model-based sonar localization for mobile robots", Robotics, Autonomous Syst., vol. 12, pp. 173-186, 1994.

[6]. C. J. Wu and C. C. Tsai, "Localization of an autonomous mobile robot based on ultrasonic sensory information," Journal of Intelligent and Robotic Systems 30, pp. 267-277, 2001.

[7]. C. C. Tsai, "A localization system of a mobile robot by fusing dead-reckoning and ultrasonic measurements," IEEE Transactions on Instrumentation and Measure- ment, vol. 47, no. 5, pp. 1399-1404, October 1998.

[8]. J. C. Hsu , "Self Location of an Autonomous Mobile Robot Using

Fuzzy Adaptive Extended Information Filtering Schemes", MS thesis, Department of Electrical Engineering, National Chung-Hsing University, July 2002.

[9]. S. W. Lai, "Multisensorial Self-Localization of an Autonomous Mobile Robot over Uneven Terrain", MS Thesis Department of Electrical Engineering, National Chung- Hsing University, June 2000.

[10]. A. M. Sabatini, "A digital signal processing techniques for compensating ultrasonic sensors", IEEE Trans. Instrum. Meas., vol. 44. no. 4, pp. 869-874, 1995.

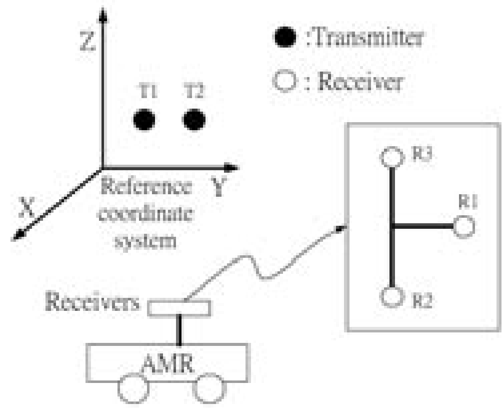

Figure 1. Physical configuration of the novel ultrasonic location system

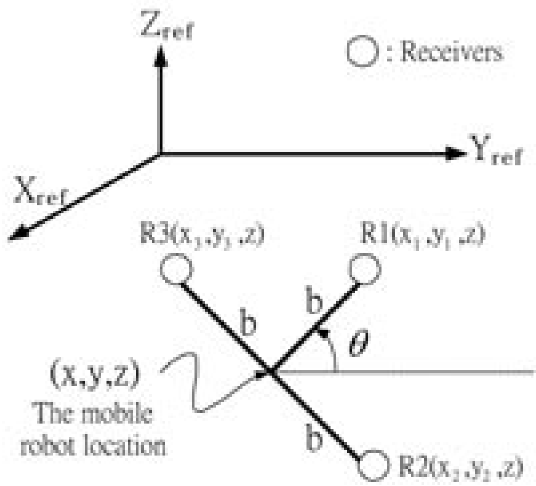

Figure 2. The geometric arrangement of the receivers

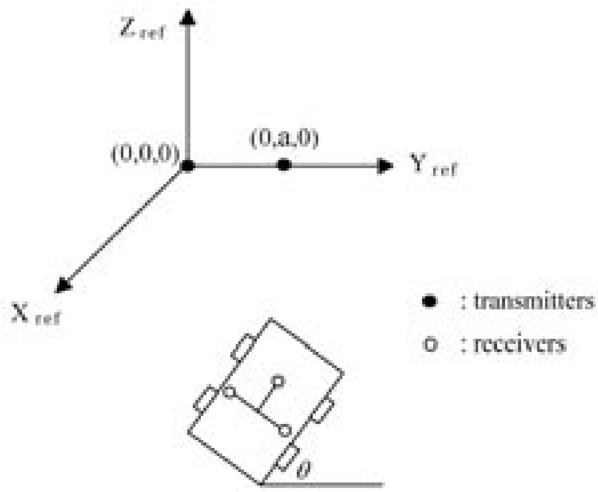

Fig 3. Two ultrasonic transmitters are installed at positions [0,0,0], [0,a,0] of the reference frame, respectively, three receivers are mounted on the AMR. Where θ is the orientation of the vehicle

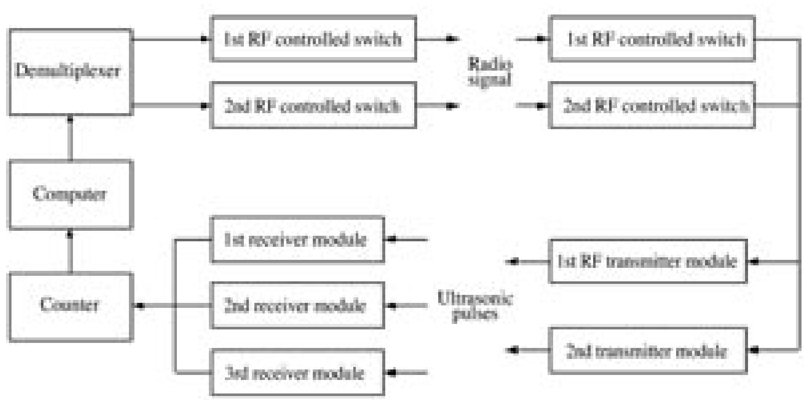

Figure 4. Block diagram of the hardware of the location system

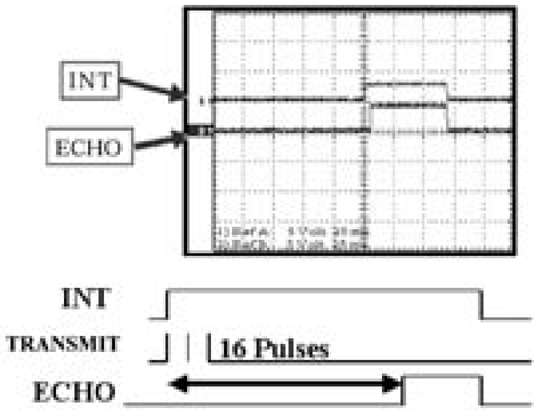

Figure 5. Single-Echo- Mode time sequential diagram

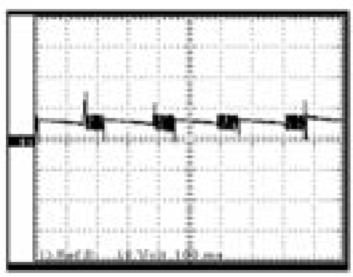

(a)

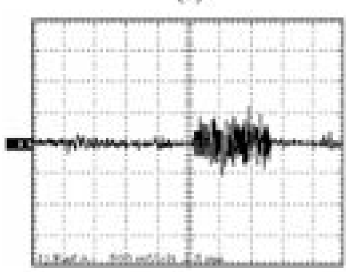

(b)

Figure 6. (a) Transmitter signal
(b) Receiver signal

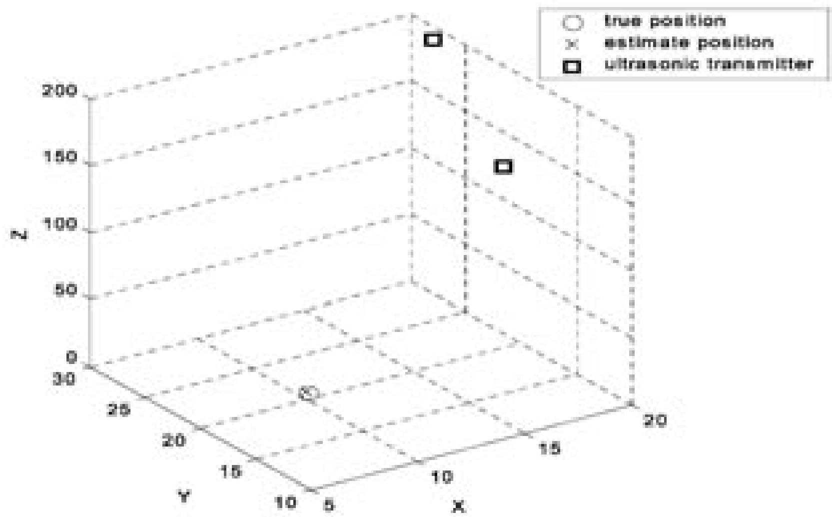

Figure 7. Comparison of the true and estimated position of the robot

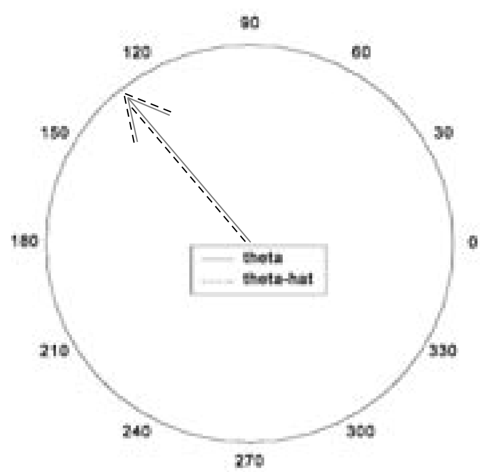

Figure 8. Comparison of the true and estimated orientation of the robot

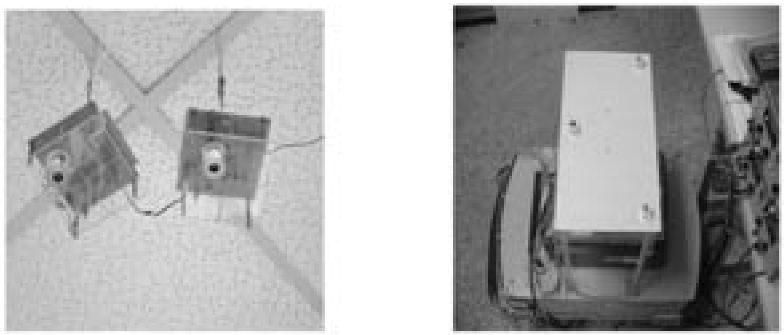

Figure 9. Pictures of the ultrasonic transmitters and receivers

Table 1. The estimation results of the static pose of the AMR

(x, y, z) cm	(0,0,46)	(0,0,46)	(0,0,46)	(0,0,46)
θ (degree)	0°	45°	90°	135°
$(\hat{x}, \hat{y}, \hat{z})$ cm	(1.04,0.02,46.01)	(0.29,0.27,45.99)	(-1.33,-0.46,45.9)	(1.2,-1.12,45.8)
$\hat{\theta}$ (degree)	1.22°	42.65°	89.04°	137.09°
$\lvert \hat{x} - x \rvert$	1.04 cm	0.29 cm	1.33 cm	1.2 cm
$\lvert \hat{y} - y \rvert$	0.02 cm	0.27 cm	0.46 cm	1.12 cm
$\lvert \hat{z} - z \rvert$	0.01 cm	0.01 cm	0.1 cm	0.2 cm
$\lvert \hat{\theta} - \theta \rvert$	1.22°	2.35°	0.96°	2.09°
(x, y, z) cm	(0,0,46)	(0,0,46)	(0,0,46)	(0,0,46)
θ (degree)	180°	225°	270°	315°
$(\hat{x}, \hat{y}, \hat{z})$ cm	(2.94,0.03,45.74)	(1.05,1.02,45.65)	(-0.03,2.0,45.78)	(-2.8,3.02,45.69)
$\hat{\theta}$ (degree)	180.65°	224.42°	270.99°	312.85°
$\lvert \hat{x} - x \rvert$	2.94 cm	1.05 cm	0.03 cm	2.8 cm
$\lvert \hat{y} - y \rvert$	0.03 cm	1.02 cm	2.0 cm	3.02 cm
$\lvert \hat{z} - z \rvert$	0.26 cm	0.35 cm	0.22 cm	0.31 cm
$\lvert \hat{\theta} - \theta \rvert$	0.65°	0.58°	0.99°	2.15°

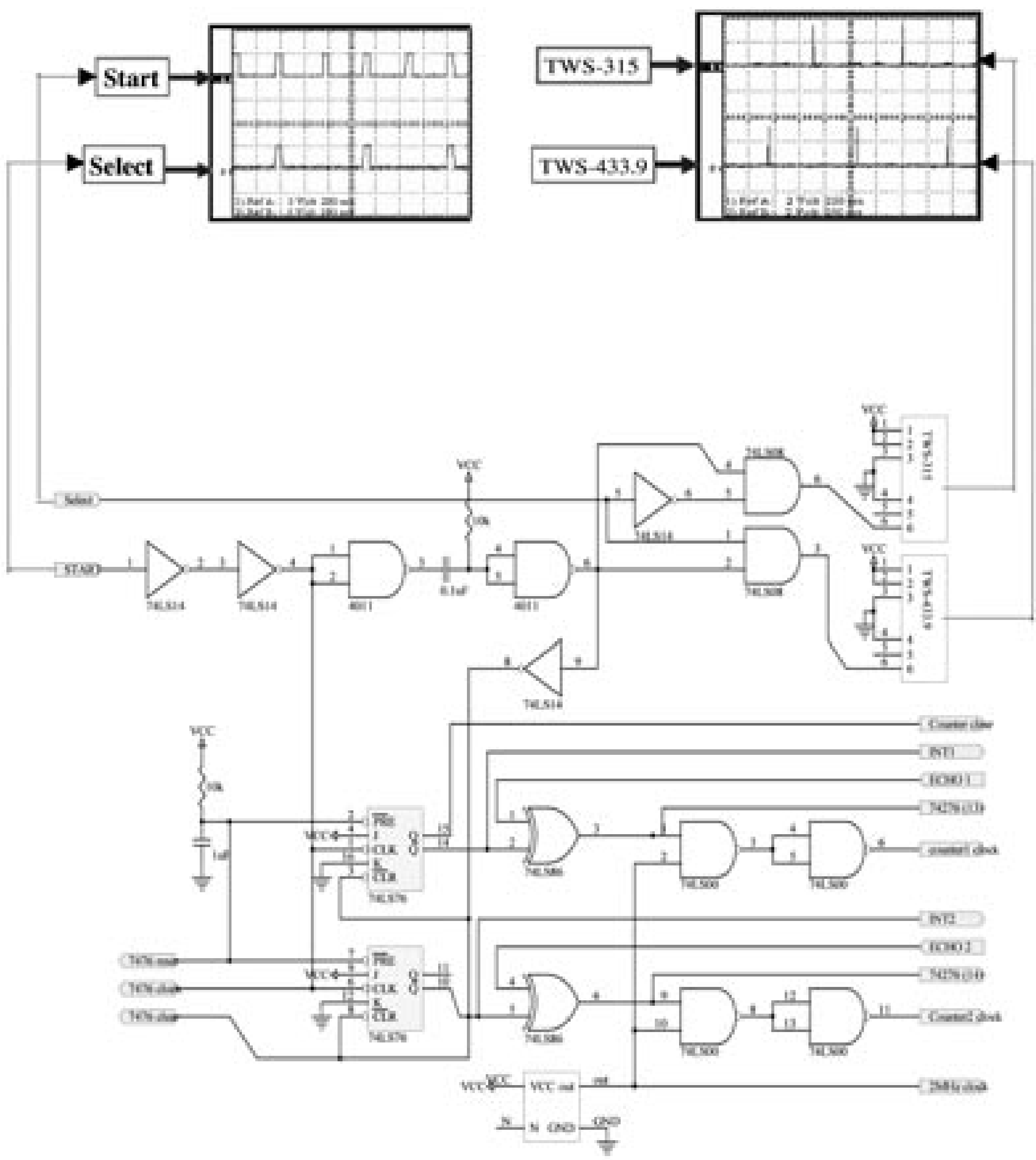

Figure 10 . The circuit diagram of the ultrasonic receiver

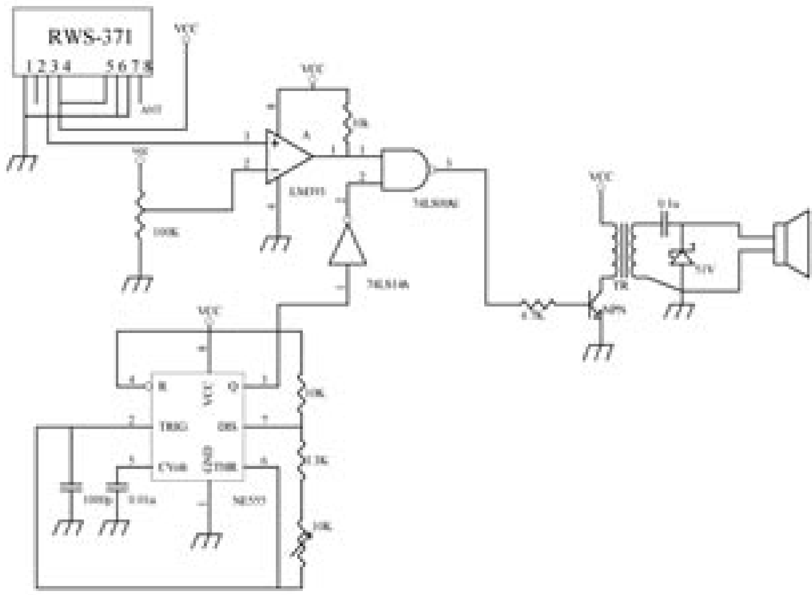

Figure 11. The circuit diagram of the ultrasonic transmitter